Merina Paul Das et al /J. Pharm. Sci. & Res. Vol. 9(12), 2017, 2553-2557

ISSN:0975-1459
Journal of Pharmaceutical Sciences and Research
www.jpsr.pharmainfo.in

Evaluation of Antibacterial Efficacy of Biogenic Zinc Oxide Nanoparticles on Cotton Fabrics

Merina Paul Das*, L. Jeyanthi Rebecca
Department of Industrial Biotechnology, Bharath University, Chennai, India

Abstract

Growing need of potent antibacterial agents has renewed a keen interest in the development of nanomaterials with antibacterial properties. The current work demonstrated the biosynthesis of zinc oxide nanoparticles (ZnO NPs) using aqueous leaf extract of *Cardiospermum halicacabum* and its bactericidal activity. The resultant biogenic metal oxide nanoparticles were analyzed by various characterization techniques. UV–vis spectrum of ZnO NPs showed characteristic band at 386 nm with band gap energy 3.21 eV. SEM and TEM analysis revealed spherical and rod shaped ZnO NPs within size range 30-80 nm for spherical, 100 nm long with 5 nm width for rod shaped and the elemental composition was studied by EDX analysis. The crystalline nature of biogenic ZnO NPs was confirmed by XRD. FTIR explained about the bioactive molecules present in the leaf extract, responsible for synthesis and stabilization of metal oxide nanoparticles. Finally, antibacterial assay was carried out to evaluate the antimicrobial property of ZnO nanoparticles coated on cotton fabrics against clinical isolates, *Escherichia coli* (Gram-negative), *Staphylococcus aureus* (Gram-positive) and the bacterial survival rates treated with NPs were evaluated using live/dead fluorescence assay. The zone of inhibition showed that ZnO NPs has significant antibacterial activities against Gram-negative bacteria than the Gram-positive strain with high selectivity. This study suggests that bacteriostatic ZnO NPs might be approached to the novel therapeutic direction by development of new antimicrobial agents in clinical practice.

Keywords: Biogenic synthesis, ZnO NPs, cotton fabric, antibacterial activity.

INTRODUCTION

Recently many nano-based materials have drawn tremendous attention as potential biocompatible and antibacterial agents as they possess broad range of activities against clinically significant pathogens [1]. Nanomaterials are known to facilitate the interaction with the bacteria due to their anionic or cationic charges present on their surfaces, high surface to volume ratio, tuneable size, density of charges etc. [2]. It have been reported that size, shape and morphology of the particles play a significant role in antimicrobial activity, smaller the particle size higher the antimicrobial property was observed [3]. Among the nanoparticles, zinc oxide nano particles (ZnO NPs) have been found to be used more often in biomedical field including quantum dots for cell trafficking [4], textile coated material as an antimicrobial agent [5], biosensing material for biomarker and heavy metal detection [6], drug delivery vehicles [7], photo catalyst [8], UV protectant in cosmetics [9], Zn nutrient supplements [10] etc. Furthermore, it is evident from the reports that these nano sized ZnO particles exhibits excellent bactericidal properties against a wide range of bacteria and its less toxic nature to human cells enables us to recommend their use in food, pharmaceutical, textile industries etc. [11-16]. The antibacterial mechanism of ZnO NPs relies on the interaction between nanoparticles with bacterial outer membrane and/or bacterial core where it enters inside the cell wall [17]. The antimicrobial activity of the particles is enhanced when coated or immobilized on the textiles [18]. Apart from biological application, ZnO NPs are also used in plastics, lubricants, cement, glass, batteries, paints, ceramics, rubber, fire retardants, and pigments.

Till date various physico-chemical approaches have been attempted to synthesize ZnO NPs including chemical reduction [19], spray pyrolysis [20], hydrothermal method [21], solvothermal method [22], and electrochemical deposition [23]. Unfortunately most of these methods are found to be expensive and associated with the hazardous chemicals posing environmental risk. In contrast, plant mediated green chemistry approach are considered as an alternate way to synthesize eco-friendly, stable, nontoxic ZnO NPs. It has been frequently reported that phytoconstituents present in plant extract can exhibit reducing and stabilizing properties in one go, which makes them advantageous over any other synthetic method and use of additional stabilizing agents. So far there is no report on the synthesis of ZnO NPs by using leaf extract of *Cardiospermum halicacabum*.

Cardiospermum halicacabum L. is a popular herbaceous plant belonging to Sapindaceae family. This medicinal plant is popularly used in the treatment of rheumatism, lumbago, earache, and fever. Medicinally it has various pharmacological activities like antioxidant, antibacterial, antipyretic, anti-diarrheal, analgesic, anticancer etc. [24]. In the present investigation, we demonstrate the biogenic synthesis of stable ZnO NPs utilizing leaf extract of *C. halicacabum* endowed with good antibacterial activities. The bactericidal studies were carried out against both Gram-positive and Gram-negative bacteria on the fabric material.

MATERIALS AND METHODS

Materials

Zinc acetate dihydrate ($Zn(CH_3COO)_2.2H_2O$), propidium iodide (PI), fluorescein diacetate (FDA) were procured from Sigma-Aldrich Chemicals and the microbiological media was purchased from Hi-Media, India with maximum purity. All the chemicals were of analytical grade and used as received. All glasswares have been sterilized before use. The chemical solutions were prepared using double distilled water. Fresh leaves of *C. halicacabum* were collected near local area of Tambaram, Chennai.

Preparation of plant extract

The leaves of *C. halicacabum* were washed thoroughly in running water and distilled water and then dried. About 5 g of powdered leaf was heated in 100 mL of distilled water at 60 °C for 15 min. After that, the suspension was cooled, filtered and stored at 4 °C for further experiments.

Synthesis of ZnO NPs using *C. halicacabum* leaf extract

The biogenic synthesis of ZnO nanoparticles was carried out using zinc acetate as described by Gnanasangeetha et al. [25]. For biosynthesis of ZnO NPs, 1mM ($Zn(CH_3COO)_2.2H_2O$) was mixed with 50 mL of plant extract and allowed to synthesize for 3-4 h in water bath at 70 °C with continuous agitation. After the incubation time, dark yellow color precipitate appeared, confirming the formation of ZnO NPs, but complete conversion to ZnO NPs takes place during drying. Before drying, the precipitate was collected and washed by centrifugation at 8,000 rpm for 10 min and finally dried at 80 °C for 3 h in oven. The pure ZnO NPs was obtained after calcination at 800 °C for 5 h in a muffle furnace.

Characterization of nanoparticles

Biological activity and toxicity of nanoparticles are mainly influenced by the physical and chemical characteristics of the particles. Hence, the biosynthesized ZnO NPs were characterized by various analytical techniques. UV–vis spectroscopy measurements were performed on double beam UV-vis spectrophotometer at 1 nm resolution between 200-700 nm. The morphology of the ZnO NPs was examined with the help of field emission scanning electron microscopy (FESEM) and transmission electron microscopy (TEM). For FTIR spectroscopy analysis, dry powder of ZnO NPs was mixed with KBr to get pellet and then this pellet was used for analysis. The FTIR spectrum was recorded by scanning in the range 350–4000 cm^{-1} in transition mode at a resolution of 4 cm^{-1}. In order to verify the crystal structure of the ZnO NPs, XRD analysis was carried out. The characterization of the purified zinc oxide nanoparticles was carried out with a powder X-ray diffractometer operated at a voltage of 40 kV and a current of 30 mA with Cu Kα radiation in a wide range of Bragg angles 2θ. The presence of elemental composition of ZnO was determined by Energy dispersive X-ray (EDX) analysis. The experiment was performed using FESEM attached EDX analyser.

Antibacterial assay

The zinc oxide nanoparticles synthesized using *C. halicacabum* leaf extract was tested for antibacterial activity by standard Kirby–Bauer disc-diffusion method using cotton fabric against pathogenic bacteria *Escherichia coli* (ATCC 25922) (Gram-negative), and *Staphylococcus aureus* (ATCC 25923) (Gram-positive) [26]. For the bactericidal study, the pre-sterile cotton cloth was dipped in 50 µg/mL of ZnO NPs suspension and hydrothermally impregnated at 600 °C for different time interval (2 h and 4h). The pure bacterial strains were sub-cultured in Luria-Bertini broth in a shaker incubator. Each pathogenic strain was swabbed uniformly on individual Muller–Hinton agar plates using sterile cotton swab and allowed to dry. Then the nanoparticle loaded cotton discs were placed on the plates. A control disc without ZnO NPs at the centre of the plate was used. The plates were incubated at 37 °C for 24 h and after the incubation, different levels of zone of inhibition was measured.

Further antibacterial activity of the ZnO NPs was reconfirmed by live/dead bacterial fluorescence viability assay using fluorescent dyes propidium iodide (PI) and fluorescein diacetate (FDA). PI is used to stain the dead cells whereas FDA is used to stain live cells. Briefly, 2 mL of overnight test bacterial culture (OD_{600} ~ 1.2) was transferred into each well of a 24 well micro titer plate. 25 µL of ZnO NPs at concentration of 50 µg/mL was added into each well and incubated in shaker incubator for 30 min. After the incubation, the cells were collected by centrifugation, washed twice with PBS buffer, and resuspended into fresh buffer in eppendorf tube. 20 µL of dye solution comprising 20 µg/mL of PI and 50 µg/mL of FDA was then added to the ZnO treated bacterial sample and incubated in dark for 15 min. Live/dead bacterial cells were observed by using fluorescence microscope.

RESULTS AND DISCUSSION

The addition of leaf extract to $Zn(CH_3COO)_2.2H_2O$ solution, the typical deep yellow color suspension formed due to chelation between zinc and bioactive molecules from plant, provided a convenient visual assessment of ZnO nanoparticle formation [27]. These colors arise due to surface plasmon resonance (SPR) excitation of the nanoparticles. Further the formation of ZnO NPs was confirmed by UV-vis spectroscopy. UV–vis spectroscopic study is an important and informative technique to elucidate the optical properties of nanoparticles [28]. Figure 1 shows the absorption spectrum of zinc oxide nanoparticles synthesized using *C. halicacabum* leaf extract. According to the spectrum, bulk ZnO produced a clear characteristic sharp absorption peak at 386 nm which can be assigned to the transition of electrons from valence band to conduction band (O_{2p}-Zn_{3d}) [29]. The band gap energy (E_g) was estimated to be 3.21 eV calculated from the equation:

$$E_g = \frac{hc}{\lambda} \text{ eV} \qquad (1)$$

where h is the Planck's constant (6.626 x 10^{-34} Js), C is the light velocity (3x10^8 m/s) and k is the wavelength (nm). In addition, the broadened SPR bands with absorption tail in the longer wavelengths might be due to the size distribution of the nanoparticles.

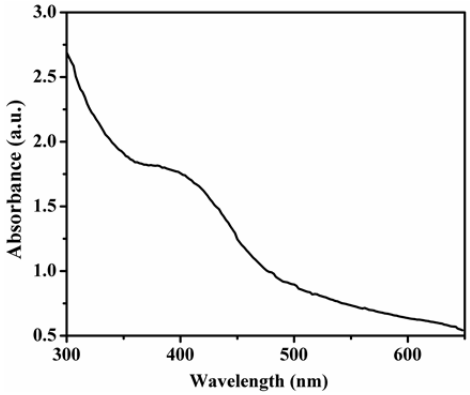

Figure 1: UV-vis absorption spectrum of ZnO NPs synthesized by using *C. halicacabum* leaf extract

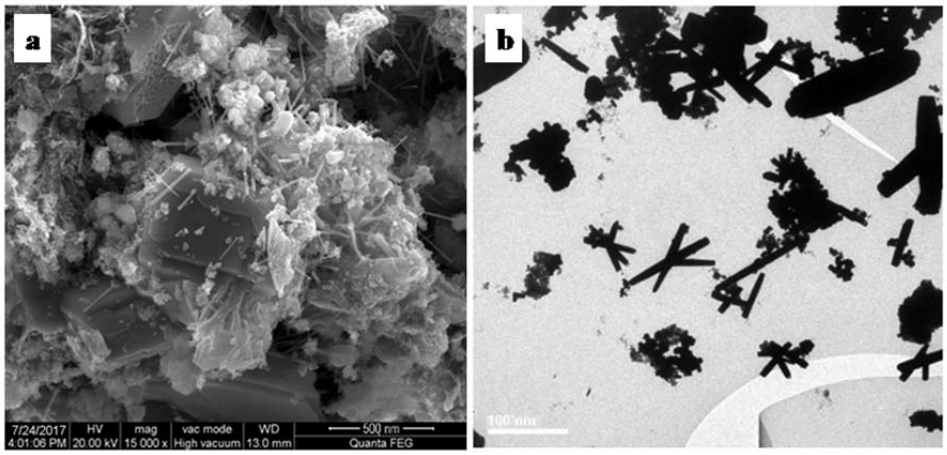

Figure 2: (a) SEM and (b) TEM micrograph of biogenic ZnO NPs

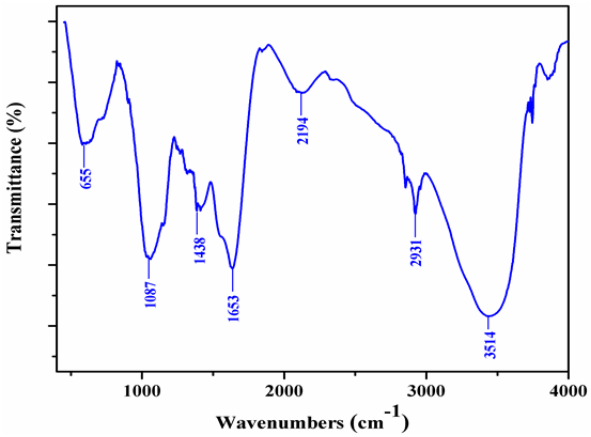

Figure 3: FTIR spectrum of zinc oxide nanoparticles synthesized by *C. halicacabum* aqueous leaf extracts

The size and morphology of biosynthesized ZnO NPs were investigated by using FESEM and TEM. The FESEM images of ZnO NPs depicted the biosynthesized particles as polydispersed and spherical in shape with little agglomeration (Figure 2a). Along with the spherical particles, nano-rods were also obtained. From the micrograph it is evident that the sizes of the particles ranges in diameter between 30-80 nm for spherical and size of the nano-rods were found in the range of 100 nm long and 5 nm width. To confirm the FESEM results, the nanosized ZnO were subjected to high magnified TEM analysis. TEM image (Figure 2b) clearly reveals the spherical and rod shaped ZnO particles, where both nanostructures were found in almost equal proportion. This observation is in accordance with the XRD results.

Figure 3 represents the FTIR transmission spectrum of zinc oxide nanoparticles synthesized by using *C. halicacabum* aqueous plant extract. The spectrum of ZnO NPs demonstrates the peaks found at 3514, 2931, 2194, 1653, 1438, 1087 and 655 cm^{-1}. The broad and intense band at 3514, 1653, 1087 cm^{-1} are assigned to O-H stretching, –C–O–C stretching and a characteristic amide I band of aromatic ring, respectively [30-32], medium absorption band at 2931, 2194 cm^{-1} corresponds to aliphatic –C–H stretching [33], 1438 cm^{-1} is owing to methylene scissoring vibrations from protein, and 655 cm^{-1} is assigned to alkynes [34]. The IR bands corresponding to bonds such as –C–H, –O–H, –C–O–C and –C–N are derived from the water soluble metabolites such as flavonoids, alkaloids and tanins present in aqueous *C. halicacabum* leaf extract [35]. FTIR results reveal that the water soluble fractions of plant extract play a crucial role in the bioreduction, stabilization, and shape fabrication of the nanoparticles.

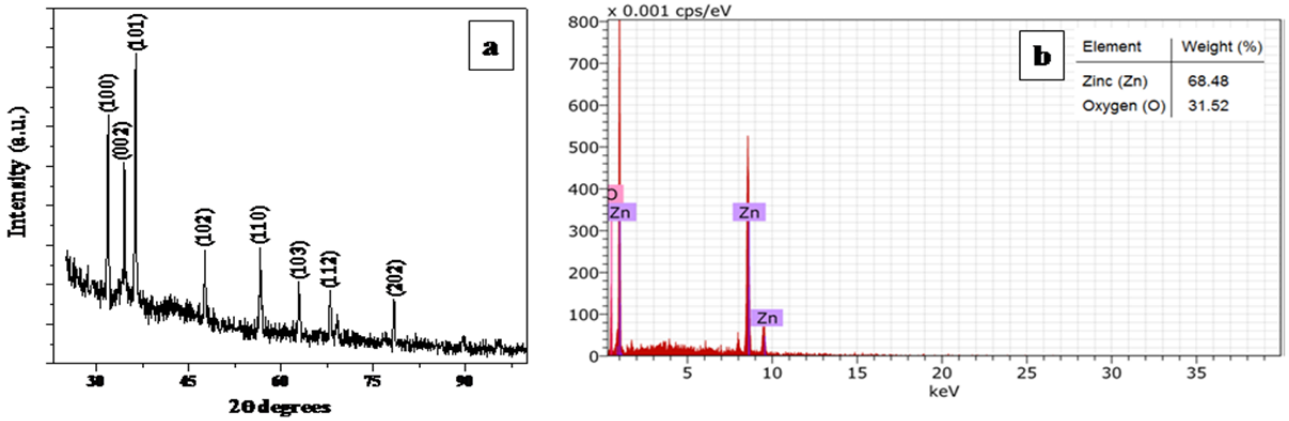

Figure 4: (a) X-ray diffraction pattern of biosynthesized zinc oxide nanoparticles and (b) Chemical constituent analysis of ZnO NPs using EDX

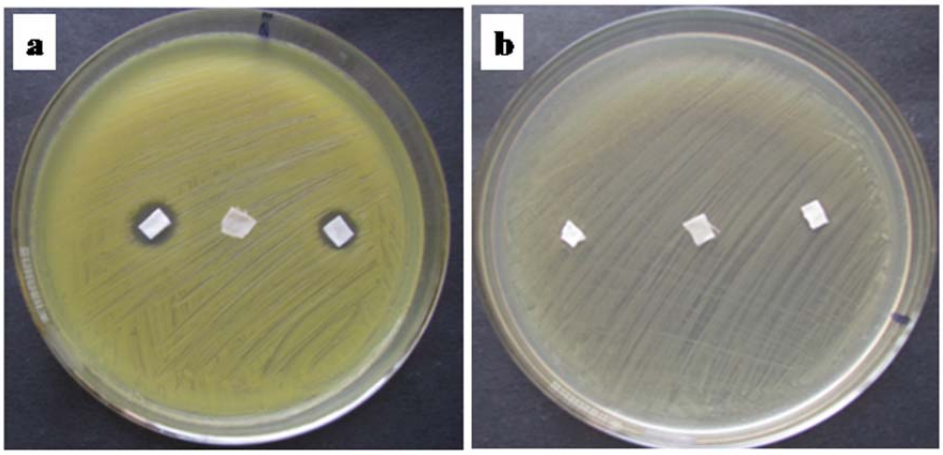

Figure 5: Antibacterial activities of ZnO NPs against (a) Gram-negative and (b) Gram-positive bacteria on fabric cloth

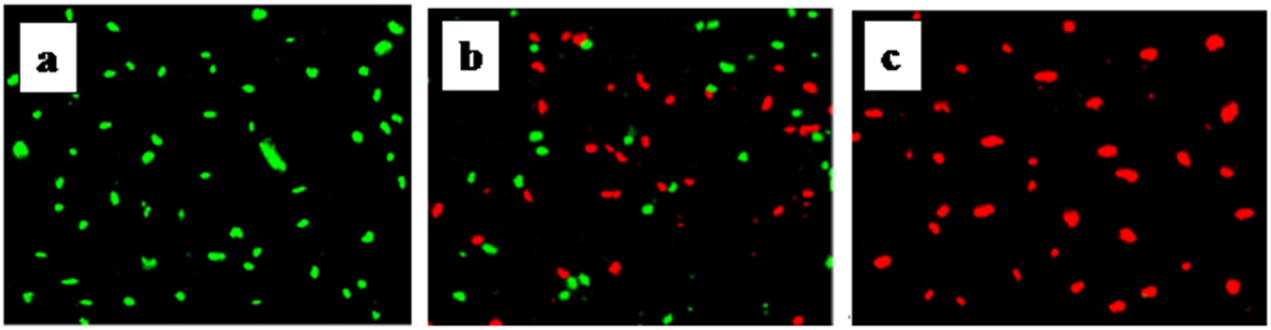

Figure 6: Fluorescence images of *E. coli* bacterial cells (a) untreated with ZnO NPs, (b) treated with ZnO NPs for 15 min and (c) treated with ZnO NPs for 30 min

Crystal nature of purified nano sized ZnO particles were evaluated using X-ray diffractometer. Figure 4a shows the XRD pattern of ZnO NPs synthesized using green chemistry approach. XRD results showed distinct diffraction peaks at 2θ values of 31.82°, 34.47°, 36.32°, 47.62°, 56.62°, 62.87°, 68.12°, and 78.37° indexed to the (100), (002), (101), (102), (110), (103), (112), and (202), respectively in crystalline planes. The lattice constant of zinc oxide was matched well with the database of Joint Committee on Powder Diffraction Standards (JCPDS) values. No additional diffraction peaks for corresponding to the precursor (zinc acetate) and/or bi-products were observed, which confirms that only pure ZnO nanoparticles were synthesized. The same result was reconfirmed by EDX analysis.

EDX pattern confirmed the presence of pure elemental zinc and oxygen of ZnO NPs without any other impurities (Figure 4b). The optical absorption peak is found at 1.1 keV, 8.5 keV, and 9.5 keV assigned to Zn L_a, Zn K_a, and Zn K_b, respectively, which is characteristic for ZnO nanocrystallites due to surface plasmon resonance [36]. The spectroscopic results revealed that the particle consisted of 68.48% Zn and 31.52% O_2.

The quantitative antibacterial activity was evaluated by measuring inhibition zone around the cotton discs against Gram-positive and Gram-negative bacteria. Figure 5 shows the bactericidal efficiency of ZnO NPs depends on the bacterial cell type as nanoparticles were more sensitive to *E. coli* (Gram-negative) bacterial growth than *S. aureus* (Gram-positive) at 50 µg/mL concentration. The mean inhibitory zone against *E. coli* was found 13 mm for 2 h incubated disc whereas 15 mm was found for 4 h incubated cloth disc (Figure 5a). The contact time between nanoparticles and the fabric material improved the antibacterial efficiency of ZnO NPs. The antibacterial activity was not observed against Gram-positive, *S. aureus* strains were not inhibited by the ZnO nanoparticles (Figure 5b). Previously it has been reported that the antibacterial mechanism of nanoparticles against Gram-positive and Gram-negative bacteria relies on the difference in the cell-membrane structural composition, most distinctively peptidoglycan layer thickness [37]. Gram-positive bacteria possess thick peptidoglycan layer composed of linear polysaccharide chain cross-linked with small peptides, forming a rigid cell membrane to penetrate ZnO NPs, thus no inhibition zone was formed, whereas the cell wall Gram-negative bacteria has thinner polysaccharide layer, showed significant bactericidal effect.

The antibacterial activity was further validated by confocal microscopic analysis using a mixture of fluorescent dyes, FDA and PI. FDA emits green fluorescence while PI emits red fluorescence from live and dead cells, respectively

under fluorescence microscope. FDA can enter directly into the live cells where it reacts with the intracellular esterase enzyme and activate fluorescence while PI can penetrate only into the cells and bind with nuclei when the cellular membrane is ruptured or damaged [38]. A large proportion of green and red fluorescence was observed in Figure 6a and c for control and treated *E. coli* bacterial cells after 30 min of incubation, respectively. After 15 min of incubation as shown in Figure 6b, the Gram-negative *E. coli* sample treated with 50 µg/mL ZnO NPs had nearly equal proportion of live and dead bacterial cells.

CONCLUSION

In conclusion, a simple, rapid green synthetic approach was adopted to synthesize biogenic ZnO nanoparticles by using aqueous leaf extract of *C. halicacabum*. UV-vis absorption spectrum showed the formation of crystalline ZnO NPs with the characteristic SPR peak. FESEM and TEM micrograph showed the nano-spherical and nano-rod shaped nanoparticles and elemental composition of ZnO was demonstrated by EDX profile. The crystalline structure and average size of ZnO NPs was confirmed with the XRD technique. Cotton fabric with ZnO NPs showed high antibacterial activity against Gram-negative bacteria than the Gram-positive one. Result of the study revealed the bactericidal properties of the metal oxide nanoparticles on the textile materials and ZnO NPs impregnation of cotton fabrics will be a useful tool as bactericidal bandage materials in hospitals.

ACKNOWLEDGEMENTS

The authors convey their thanks to Department of Industrial Biotechnology, Bharath University, Chennai, for providing laboratory facilities and encouragement. The author also acknowledges Department of Nanotechnology, SRM University, Chennai for providing necessary facilities.

REFERENCES

[1] Neal, A. L., *Ecotoxicol*. 2008, *17*, 362 – 371.
[2] Kishen, A., Shi, Z., Shrestha, A., Neoh, K. G., *J. Endod*. 2008, *34*, 1515 – 1520.
[3] Morones, J. R., Elechiguerra, J. L., Camacho, A., Holt, K., Kouri, J. B., Yacaman, M. J., *Nanotechnology* 2005, *16*, 2346 – 2353.
[4] Gao, P. X., Ding, Y., Mai, W. J., Huges, W. L., Lao, C. S., Wang, Z. L., *Science* 2005, *309*, 1700 – 1704.
[5] Xu, S., Qin, Y., Xu, C., Wei, Y., Yang, R., Wang, Z. L., *Nat. Nanotechnol*. 2010, *5*, 366 – 373.
[6] Wang, Z. L., Song, J., *Science* 2006, *312*, 242 – 246.
[7] Rasmussen, J. W., Martinez, E., Louka, P., Wingett, D. G., *Expert Opin. Drug Deliv.* 2010, *7*, 1063 – 1077.
[8] Anbuvannan, M., Ramesh, M., Viruthagiri, G., Shanmugam, N., Kannadasan, N., *Spectrochim. Acta A Mol. Biomol. Spectrosc.* 2015, *15*, 304 – 308.
[9] Smijs, T. G., Pavel, S., *Nanotechnol. Sci. Appl.* 2011, *4*, 95 – 112.
[10] Swain, P. S., Rao, S. B. N., Rajendran, D., Dominic, G., Selvaraju, S., *Anim. Nutr*. 2016, *2*, 134 – 141.
[11] Jones, N., Ray, B., Ranjit, K. T., Manna, A. C., *FEMS Microbiol. Lett*. 2008, *279*, 71 – 76.
[12] Jalal, R., Goharshadi, E. K., Abareshi, M., Moosavi, M., Yousefi, A., Nancarrow, P., *Mater. Chem. Phys*. 2010, *121*, 198 – 201.
[13] Seil, J. T., Webster, T. J., *Int. J. Nanomedicine*. 2012, *7*, 2767 – 2781.
[14] Emami-Karvani, Z., Chehrazi, P., *Afr. J. Microbiol. Res.* 2011, *5*, 1368 – 1373.
[15] Raghupathi, K. R., Koodali, R. T., Manna, A. C., *Langmuir* 2011, *27*, 4020 – 4028.
[16] Uikey, P., Vishwakarma, K., *Int. J. Emerg. Technol. Comput. Sci. Electron*. 2016, *21*, 239 – 242.
[17] Seil, J. T., Webster, T. J., *Int. J. Nanomedicine*. 2012, *7*, 2767 – 2781.
[18] Abramov, O.V., Gedanken, A., Koltypin, Y., Perkas, N., Perelshtein, I., Joyce, E., Mason, T. J., *Surf. Coat. Technol*. 2009, *204*, 718 – 722.
[19] Delamar, M., Desarmot, G., Fagebaume, O., Hitmi, R., Pinson, J., Savenat, J. M., *Carbon* 1997, *35*, 801 – 807.
[20] Sun, R. D., Nakajima, A., Fujishima, A., Watanabe, T., Hashimoto, K., *J. Phys. Chem. B* 2001, *105*, 1984 – 1990.
[21] Olson, D. C., Shaheen, S. E., Collins, R. T., Ginley, D. S., *J. Phys. Chem. C* 2007, 111, 16670 – 16678.
[22] He, Z., Que, W., *J. Nanoeng. Nanomanuf*. 2012, *2*, 17 – 21.
[23] Gan, X., Gao, X., Qiu, J., Li, X., *Appl. Surf. Sci*. 2008, *254*, 3839 – 3844.
[24] Das, M. P., Yasmine, Y., Vennila Devi, P., *Int. J. Pharm. Bio. Sci.* 2015, *6*, 711 – 719.
[25] Gnanasangeetha, D., Thambavani, D. S., *J. Chem. Biol. Phys. Sci*. 2013, *4*, 238 – 246.
[26] Laldhas, K. P., Cheriyan, V. T., Puliappadamba, V. T., Bava, S. V., Unnithan, R. G., Vijayammal, P. L., Anto, R. J., *J. Cell. Mol. Med*. 2010, *14*, 636 – 646.
[27] Selvarajan, E., Mohanasrinivasan, V., *Mater. Lett.* 2013, 112, 180 – 182.
[28] Rajabi, H. R., Farsi, M., *Mater. Sci. Semicon. Proc*. 2016, *48*, 14 – 22.
[29] Harish, K., Renu, R., *Int. Lett. Chem. Phys. Astron*. 2013, *14*, 26 – 36.
[30] Das M. P., Livingstone J. R., Veluswamy, P., Das, J., J. Food Drug Anal. 2017, 1 – 9. http://dx.doi.org/10.1016/j.jfda.2017.07.014.
[31] Edwards, H. G. M., Falk, M. J., Sibley, M. G., Alvarez-Benedi, J., Rull, F., *Spectrochim. Acta A* 1998, *54*, 903 – 920.
[32] Gole, A., Dash, C., Ramakrishnaan, V., Sainkar, S. R., Mandal, A. B., Rao, M., Sastry, M., *Langmuir* 2001, *17*, 1674 – 1679.
[33] Chowdhury, J., Ghosh, M., *J. Colloid Interface Sci*. 2004, *277*, 121 – 127.
[34] Caruso, F., Furlong, D. N., Ariga, K., Ichinose, I., Kunitake, T., *Langmuir* 1998, *14*, 4559 – 4565.
[35] Das, M. P., Yasmine, Y., Devi, P. V., *Int. J. Pharm. Bio. Sci*. 2015, *6*, 711 – 719.
[36] Bahadur, H., Srivastava, A. K., Sharma, R. K., Chandra, S., *Nanoscale Res. Lett*. 2007, *2*, 469 – 475.
[37] Shrivastava, S., Bera, T., Roy, A., Singh, G., Ramachandrarao, P., Dash, D., *Nanotechnology* 2007, *18*, 225103 – 225111.
[38] Netuschil, L., Auschill, T. M., Sculean, A., Arweiler, N. B., *BMC Oral Health* 2014, *14*, 2.